Desalination and Water Treatment
www.deswater.com
doi: 10.1080/19443994.2013.808431

52 (2014) 390–400
January

Taylor & Francis
Taylor & Francis Group

Advanced treatment of refractory sebacic acid wastewater

Chetan Chavhan, Pranav Tripathi, Nageswara Rao Neti*

National Environmental Engineering Research Institute (Council of Scientific & Industrial Research) Nehru Marg, Nagpur 440020, India
Tel. +91 712 224986 88 402; Fax: +91 712 2249900; email: nn_rao@neeri.res.in

Received 11 April 2012; Accepted 30 January 2013

ABSTRACT

Advanced treatment of refractory sebacic acid (SA) present in wastewater discharges from SA manufacturing industry (SAWW) is reported. Ion exchange (IE), electrochemical oxidation (EO), EO coupled with electrocoagulation (EO–EC), wet air oxidation (WAO), and catalytic wet air oxidation (CWAO) experiments were conducted. It is found that SA can be efficiently removed from aqueous solutions using a strong base anion-exchange resin (Amberlite IR 400), which showed a breakthrough capacity of 49.0 mg SA/mL resin (0.485 meq/mL). However, presence of inorganic anions (SO_4^{2-}, PO_4^{2-}, Cl^-, and NO_3^-) is detrimental. Regeneration and reuse of spent resin, the effect of inorganic anions and morphology (SEM) of spent resin were also investigated. In addition, batch EO experiments conducted using Ti/RuO_2-Pt anode and stainless steel (SS) cathode showed poor mineralization efficiency (8.4%). Pd^{2+}-catalyzed WAO experiments performed in a high pressure reactor (473 K, 0.689 MPa, 2 h) provided more efficient mineralization of SA (42.2%) compared with EO. The results constitute an important outcome which may be useful to SA manufacturing industry.

Keywords: Sebacic acid; Ion-exchange; Electrooxidation; Catalytic wet air oxidation; Mineralization

1. Introduction

Sebacic acid (SA), (decanedioic acid, HOOC–$(CH_2)_8$–COOH) is a valuable raw material for production of nylon, alkyd resins, plasticizers, lubricants, cosmetics, and pharmaceuticals [1]. Nevertheless, there are concerns regarding its hazardous health effects and acute toxicity. Oral ingestion tests on rats revealed the acute oral toxicity (LD_{50}) to be 6,000 mg/kg rat [2]. Though specific information on its ecological toxicity is scarce, the products of its biodegradation are reported to be more toxic [2]. The health and ecological concerns associated with SA assume significance in view of its solubility in water ~0.10 g/100 ml [3].

Presently, SA is manufactured from the caustic fusion of castor oil [4]. Highly saline (TDS = 82,000 mg L^{-1}) liquid effluent, which contains high concentrations of SA (~300 mg L^{-1}) and phenol (2,500–3,000 mg L^{-1}), is

*Corresponding author.

Presented at the DAE—BRNS Biennial Symposium on Emerging Trends in Separation Science and Technology (SESTEC 2012) Mumbai, India, 27 February–1 March 2012

discharged. Further, it was observed that SA does not undergo degradation through physicochemical and biological treatment processes in a conventional effluent treatment plant [5]. Though many methods have been investigated for the remediation of phenol-containing effluents including SA manufacturing wastewater [6,7], there are no reported studies on the treatment aiming at SA removal and degradation. We attempted SA removal using ion-exchange (IE), and its degradation using electrochemical oxidation (EO), EO coupled with Electrocoagulation (EC), wet air oxidation (WAO), and catalytic wet air oxidation (CWAO) processes. The results suggest that ion-exchange method is applicable to remove SA from its neat aqueous solutions, while the presence of inorganic anions such as SO_4^{2-}, NO^{2-}, HPO_4^{2-}, and Cl^- is detrimental. On the other hand, CWAO is found to be moderately efficient for oxidative treatment of simulated SA wastewater.

2. Materials and methods

2.1. Materials

Amberlite IRA-400 (Cl^- form), strongly basic anion-exchange resin, was supplied by E.Merck India Pvt. Ltd., (Mumbai). Commercially available 60% $PdCl_2$ supplied by Loba Chemical Pvt. Ltd., Mumbai, was used. SA (SA, 99.5%) was supplied by M/s Jayant Organics & Derivatives Ltd., Baroda, India. Reagent grade H_2SO_4, NaOH, NaCl, Na_2SO_2, and $AgNO_3$, were used. Deionized water (Millipore Elix 3) was used for preparing reagent solutions, as well as for resin washing.

2.2. Preparation of stock solutions

2.2.1. Stock aqueous SA solution

Stock SA solution was prepared by adding 7.0 g SA in 70 L deionized water. The filtered solution was further diluted to 70 mg/L using deionized water.

2.2.2. Simulated sebacic acid waste water (SAWW)

Type 1: Approximately 0.4 g Na_2SO_4 was mixed in 1 L of the above stock solution and the mixture is referred as simulated sebacic acid waste water (SAWW). This was used for CWAO studies.

Type 2: Type 1 wastewater was modified with 4 g NaCl. This wastewater was used for electrooxidation experiments. NaCl served as an electrolyte and a source for Cl_2/OCl^- redox couple [8].

Phenol, another major pollutant in SAWW, was not added to Type 1 and 2 wastewater, since the objective of this study is to investigate the removal/degradation of SA and the presence of phenol would obscure the TOC results.

2.3. Procedure for setting up ion-exchange column and ion-exchange experiments

A glass column (height, 30 cm, Ø1 cm) having glass wool plug at the bottom was used for packing the ion-exchange resin. The specifications of column, resin, resin bed, and flow rate are compiled in Table 1. About 4.0 g resin suspension in water was poured into the glass column. The resin was washed with 0.1 N NaOH, whereby OH^- replaced Cl^- ion from the resin. Washing with DI water was continued till no Cl^- was detected in the eluent (tested with $AgNO_3$) and till neutral pH, prior to commencing ion-exchange experiment.

Ion-exchange experiment involved passing 70 mg/L SA solution, corresponding to 46.5 ± 1.7 mg/L initial total organic carbon (TOC), through the resin bed (OH^- form). The aqueous SA solution was fed downward into the column (flow rate of 3.0 ml min^{-1}). The eluent samples were collected periodically and a total of 1,500 bed volumes of eluent (~12.3 L) were collected. After every six bed volumes, the eluent sample was analyzed for TOC. The normalized TOC concentration was

Table 1
The specifications of column, resin, resin bed, and flow rate

Column/resin/resin bed	Specification
Glass column	
Column material	Glass (Borosil)
Column height	30 cm
Internal diameter	1.0 cm
Resin	
Resin type	Amberlite IRA 400 strong base anion exchange resin
Functional group	R_3N^+
Polymer matrix	Polystyrene DVB
Ionic form	Cl^-
Exchange capacity	⩾1.40 meq/mL
Effective size	0.3–0.8 mm
Resin bed	
Height of resin bed	10.4 cm
Diameter	1.0 cm
Weight of resin	4.0 g
Bed volume	8.2 ml
Packing density	0.49 g/ml
Effluent	70 ± 2 mg/L aqueous SA solution
Flow rate	Downward 3.0 mL/min

plotted against the number of bed volumes of eluent collected to establish the breakthrough curves (BTC).

2.3.1. Procedure for regeneration of resin bed

Spent resin bed was regenerated *in situ* by passing 25 mL of 0.1 N NaCl solution. Then, the Cl^- form of resin was converted into OH form using 0.1 N NaOH, and washed with deionized water. In an alternative approach, the resin bed was removed from glass column and subjected to *ex situ* regeneration using 0.1 N NaCl.

2.3.2. Effect of anions on the ion-exchange process for SA removal

The effect of sulfate, phosphate, nitrate, and chloride ions on the ion-exchange process for SA removal was investigated. For this purpose, 15 L aqueous SA solutions (70 mg/L) containing 6.0 g each of corresponding sodium salts were added to obtain 400 mg salt/L concentration (SO_4^{2-}, 4.16 mmol/L; HPO_4^{2-}, 4.20 mmol/L; NO_3^-, 13.3 mmol/L, and Cl^-, 11.2 mmol/L). Further, the effect of SO_4^{2-} concentration in the range 30 mg/L (0.31 mmol/L)–120 mg/L (1.25 mmol/L) was also evaluated. The concentration of SA eluted in the regeneration experiments was determined using titrimetric method (section 2.7 (i)).

2.4. Procedure for electrochemical oxidation

Batch electrooxidation experiments were conducted in a cylindrical single-compartment reactor using Ti/RuO_2-Pt anode (10 cm × 10 cm) and stainless steel (SS) cathode (10 cm × 10 cm). The electrodes were positioned vertically and parallel to each other about 1 cm apart in the reactor. The electrodes were connected to a regulated DC power supply. Approximately 2 L of Type 2 wastewater was taken into the reactor, and air was bubbled using an aquarium aerator to facilitate mixing. The reaction was carried out at 3A and 16 V for 2 h and test samples were collected at 30-min intervals. The TOC was determined as a function of treatment time.

2.5. Electro coagulation coupled electrochemical oxidation

The electro coagulation (EC) experiments were performed in a laboratory-scale Plexiglas reactor (20 cm × 16 cm × 5.5 cm) comprising a sacrificial Al anode (10 cm × 10 cm) and SS cathode (10 cm × 10 cm). A typical experiment was performed on 1 L of Type 2 wastewater at 1A and 12 V, for 2 h. The treated effluent from this experiment was transferred to electrooxidation reactor and the experiment was conducted as described in Section 2.4. The TOC was determined as a function of treatment time.

2.6. Procedure for (catalytic) wet air oxidation

WAO experiments were performed using 0.5 L of Type 1 wastewater in a 1 L High Pressure SS Reactor (Model No. 1300, Amar Equipment Pvt. Ltd., Mumbai). The reactor was pressurized using air to 0.689 MPa, while the reaction mixture was stirred (200 rpm). In a CWAO experiment, 4.8 mg Pd^{2+} (8 mg of 60% $PdCl_2$) was introduced as catalyst. The reaction was carried out at 473 K for 2 h and test samples collected at 30-min intervals were analyzed for TOC.

2.7. Analytical procedure for determination of SA

The concentration of SA was determined using two analytical methods: (1) Titrimetric method and (2) TOC analysis.

(1) *Titrimetric method*: The concentration of SA in neat aqueous solutions was determined by titration using calibrated NaOH solution and phenolphthalein (pH 8.0–9.8) indicator [1]. The pH values of solution were made with digital pH meter (WTW series pH Inolab 720) and pH electrode Sentix 81, which has pH measurement accuracy ± 0.01.

(2) *TOC analysis*: The TOC in the standard solutions of SA (45, 50, 60, and 70 mg/L), as well as in test samples was determined using TOC Analyzer (Shimadzu TOC-V_{CPH}). The measurements were made in duplicate, and the standard error in TOC measurement was about ±2.0%. The concentration of SA determined by the methods (i) and (ii) agrees within an error of ±6–13%. The TOC data obtained was used for preparing breakthrough plots.

The chemical oxygen demand (COD) and biochemical oxygen demand ($BOD_{5d,\ 20^\circ C}$) exerted by SA were determined according to Standard Methods [9].

2.8. SEM

The surface morphology of virgin, used resin particles with and without deposition on the surface, and cross-sections were examined using scanning electron microscopy (SEM) (JEOL JXA84OA).

3. Results and discussion

3.1. TOC, COD, BOD of SA

SA is a saturated dibasic acid. Information on COD and BOD parameters that indicate its ecological toxicity does not exist. Therefore, it is considered important to generate this data. The TOC, COD, and BOD of SA solutions (30–70 mg/L) were determined. The observed linear correlation of TOC, COD, and BOD with the SA concentrations can be written as:

$$[\text{TOC, mg/L}] = 0.625 \times [\text{SA, mg/L}], \quad r^2 = 0.99$$

$$[\text{COD, mg/L}] = 3.17 \times [\text{SA, mg/L}], \quad r^2 = 0.98$$

$$[\text{BOD, mg/L}] = 0.37 \times [\text{SA, mg/L}], \quad r^2 = 0.94$$

The COD/TOC ratio is an important tool in the evaluation of wastewater treatment. A high COD/TOC ratio indicates presence of organic compounds that are easily oxidized by dichromate [10]. In the present case, this ratio was found to be in the range 4.50–5.18, which implies easy oxidation of SA by dichromate. On the other hand, the biodegradability index (BOD/COD) ratio [11], which indicates biodegradability of organic matter in wastewater; is in the range 0.10–0.16. This indicates poor biodegradability of aqueous SA solutions. Further, the ratio is smaller at higher SA concentrations and higher at smaller SA concentrations, indicating that ecotoxicity may set in at higher SA concentrations.

3.2. Ion-exchange process

The specifications of column, resin, resin bed, and flow rate are given in Table 1. The BTC depicting the variation of normalized TOC concentration vs. the number of eluent bed volumes are presented in Fig. 1. After each cycle of operation, the bed was regenerated as described in Section 2.3.1 and is reused. Cycle 2 represents reuse of *in situ* regenerated resin bed. Cycle 3 represents reuse of *ex situ* regenerated resin bed, and cycle 4 represents reuse of *in situ* regenerated resin bed.

The BTC corresponding to cycle 1 shows a plateau until breakthrough point at 700 bed volumes (BV, 8.2 mL). This implies that about 5.75 L eluent having zero TOC was collected prior to attaining the breakthrough point. The breakthrough capacity is found to be 49 mg SA/mL resin (0.485 meq/mL). Thereafter, the TOC concentration in the eluent samples increased gradually, suggesting gradual saturation of resin bed which continued up to about 1,350 BV. A plateau signifying complete saturation of the bed was obtained thereafter.

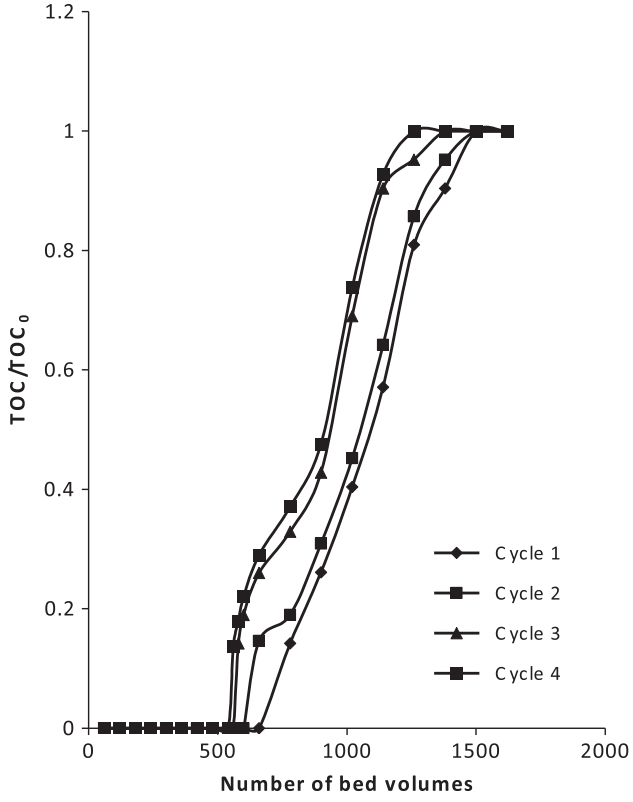

Fig. 1. BTC depicting the variation of normalized TOC concentration vs. the number of eluent bed volumes. Cycles 1–4 illustrate reusability of resin bed after either *in situ* or *ex situ* regeneration.

The physical and chemical stability of the resin bed over several regeneration–reuse cycles assumes significance when the column is intended for industrial use. Therefore, estimation of "degree of use" of the column was done as per the reported graphical method [12] and using the following relation:

$$\text{Degree of use } (\%) = A1/(A1 + A2) \times 100 \quad (1)$$

where A1 is the area over the initial plateau region of BTC, and A2 is the area over the rising section of the curve. On the basis of the graphical area estimation illustrated in Fig. 2, the degree of use is calculated to be 65.4%. This corresponds to maximum volume of eluent having zero concentration of solute that can be collected using the defined column and resin bed in

comparison with the total volume that can be collected till complete saturation of the resin bed.

The resin bed was tested for its reusability after regenerating the bed *in situ* (Cycle 2, Fig. 1). It is found that the corresponding BTC was similar to that of cycle 1, indicating excellent reuse efficiency after regeneration. After the Cycle 2, the resin was removed and regenerated *ex situ* and repacked into column. Cycle 3 represents BTC with the reuse of *ex situ* regenerated resin bed. It is noticed that the curve shifted more towards lower bed volumes compared with the BTC of cycles 1 and 2. However, the BTC of cycle 4 corresponding to reuse of *in situ* regenerated resin bed is similar to that of cycle 3, which indicates that *in situ* regenerated resin bed shows consistently good exchange capacity. The positioning of BTC of cycles 3 and 4 towards left, relative to cycles 1 and 2 may be explained on the basis of material loss that occurred during *ex situ* regeneration performed after cycle 2. There was about 0.7 g loss of resin material from the initial 4.0 g, accounting for 17% material loss. Thus, the BTC of cycles 3 and 4 actually correspond to 3.3 g resin bed.

The difference in degree of use of column between cycle 2 and cycle 1 (Fig. 2) was small (2%), which indicates that *in situ* regeneration is preferred. A few resin particles in the bed appeared grayish on careful observation, which may be due to deposition of dirt on the resin particles. This observation prompted us to examine the morphology of resin particles. The SEM photomicrographs of virgin and used resin particles with and without deposition on the surface, and cross-sections are given in Fig. 3. The virgin resin particles are spherical, though their diameter seems to differ widely ("a") and surface is fairly smooth ("b"). However, the grayish opaque particles retrieved from used-resin bed also displayed smooth surface as in photomicrograph "c", but they also exhibit extraneous deposits (photomicrograph "d"). However, these are localized deposits and do not cover entire surface of resin particles. Such extraneous deposits can potentially hamper the resin's exchange capacity. It seems that the bulk of the resin particle is also affected upon prolonged use in column. The photomicrographs "e" and "f", which correspond to cut surfaces exposing bulk pores of a virgin particle and a retrieved resin particle from the used resin bed respectively, indicate that there was a decrease in porosity of resin particles upon prolonged use.

3.2.1. Resin regeneration and recovery of SA

Complete saturation of the resin bed with SA was obtained after about 1,350 BV (Cycle 1, Fig. 1). This corresponds to exchange of 560 mg SA from 8.0 L of feed solution. We attempted to recover the exchanged SA by passing 50 mL 0.1 N NaCl through the used resin bed. The concentration of SA in the eluted brine solution determined by method (i) was 510 mg, as against expected 560 mg. Thus, 91.0% of exchanged SA could be recovered.

3.2.2. Effect of anions

As mentioned earlier, the real SAWW contains sodium sulfate. Such sources of anions can strongly influence the uptake of SA by the resin. Therefore, we attempted to understand the effect of common anions

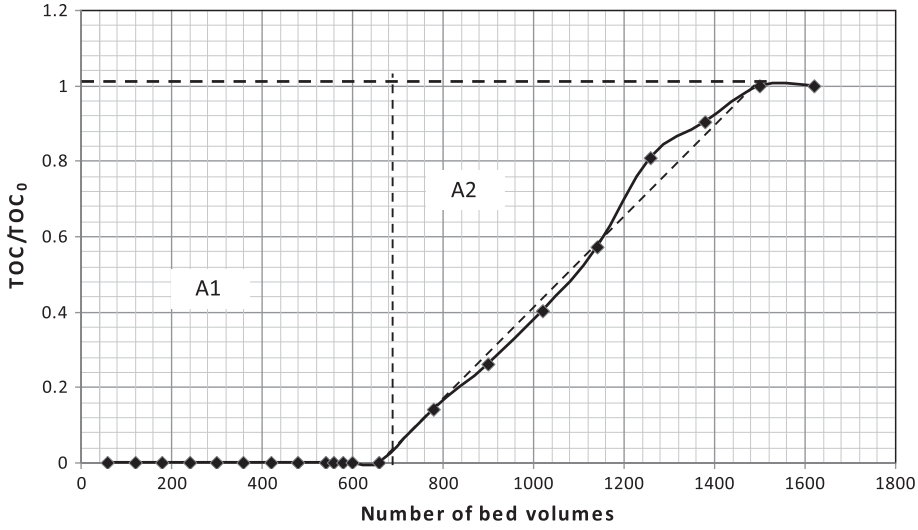

Fig. 2. Graphical method for calculating "degree of use" of resin bed. A1, area over the initial plateau region of BTC; A2, area over the rising section of the BTC.

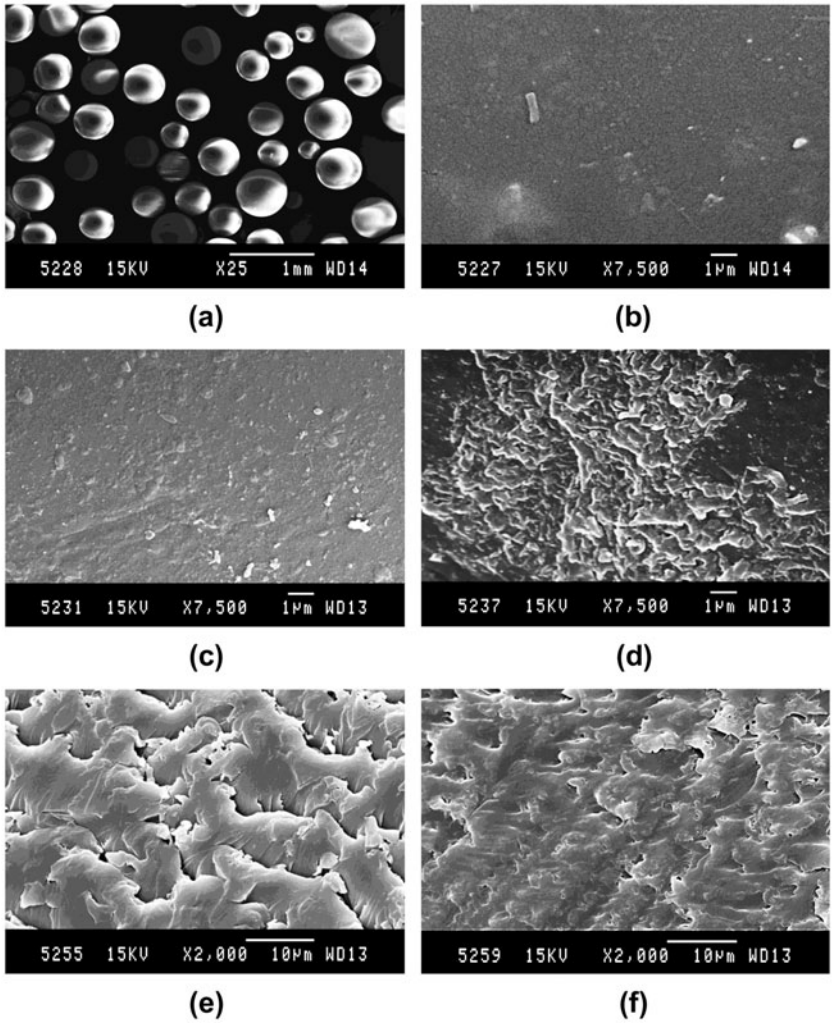

Fig. 3. SEM photomicrographs showing morphology of (a) virgin resin particles, (b) smooth surface of a virgin resin particle, (c) surface of the regenerated resin particle (end of Cycle 4), (d) view of surface deposit on the regenerated resin particle (end of Cycle 4), (e) shows bulk pores on the cut section of virgin resin particle, and (f) shows loss of bulk pores on the cut section of used resin particle.

in industrial effluents, viz., sulfate, phosphate, nitrate, and chloride on the SA removal. Accordingly, the ion-exchange experiments targeting removal of SA in the presence of arbitrary concentration of 400 mg sodium salt/L were conducted. The effective concentration of counter anions were as follows: SO_4^{2-}, 4.16 mmol/L; HPO_4^{2-}, 4.20 mmol/L; NO_3^-, 13.3 mmol/L; and Cl^-, 11.2 mmol/L). The percent inhibition by the anions was estimated by determining the concentration of SA eluted with 0.1 N NaCl (Section 3.1.1). The data is given in Table 2, while representative BTC obtained in the presence and absence of sulfate ions are shown in Fig. 4. Both divalent (SO_4^{2-} and HPO_4^{2-}) and monovalent (NO_3^- and Cl^-) ions strongly inhibit the SA removal by ion-exchange process, and only very small amount of SA in the range 0.03–0.12 g was recovered, as against expected 0.510 g. Therefore, the percent inhibition of SA uptake in presence of anions is very high ranging from 76.5 to 94.1%.

The sulfate anion concentration was varied in the range 30 mg/L (0.31 mmol/L)–120 mg/L (1.25 mmol/L) and SA recovery was once again determined. Fig. 4 (inset) depicts plot between the concentrations of recovered SA per gram of resin vs. the concentrations of sulfate anion. It can be seen that only 20% of the expected 0.51 g SA could be recovered already at the lowest sulfate concentration applied (0.31 mmol/L). The recoveries are further reduced as the sulfate concentration increased. The result confirms that it would not be feasible to remove SA from real wastewater by ion-exchange process using Amberlite IRA 400 strong base anion-exchange resin. On the other

Table 2
Effect of anions expressed as percent inhibition of the ion-exchange process for SA removal

Anion	Anion concentration (mmol/L)	Amount of recovered SA (g)	% ? Inhibition*
Anion absent	–	0.51	–
Sulphate	4.1	0.03	94.1
Phosphate	4.2	0.07	86.3
Nitrate	13.3	0.09	82.3
Chloride	11.3	0.12	76.5

*% Inhibition = 1/100 (Amount of recovered SA (g) in the absence of anion – Amount of recovered SA (g) in the presence of anion)/(Amount of recovered SA (g) in the absence of anion).

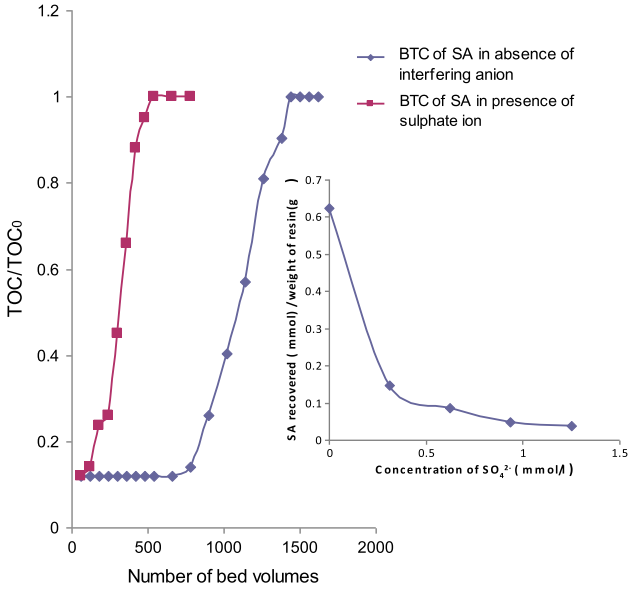

Fig. 4. BTC obtained in the presence and absence of SO_4^{2-} (400 mg/L). (Inset) Effect of concentration of SO_4^{2-} on the amount of SA recovered.

hand, removal of inorganic ions, such as NO_3^- and PO_4^{3-}, using suitable ion-exchange resins has been an attractive approach to prevent water pollution [13].

3.3. Mineralization of the stimulated SAWW using different AOPs

Since the presence of inorganic anions in SAWW is detrimental to ion-exchange of SA molecules, we attempted other methods viz., EO, EC, and (catalytic) wet air oxidation (CWAO and WAO) for its treatment. These methods are often implicated for wastewater treatment, especially when the effluents contain recalcitrant substances [14]. Fig. 5 depicts the observed percent mineralization (TOC_0–TOC_t/TOC_0) obtained through EO, EC, and (catalytic) wet air oxidation (CWAO and WAO) experiments as a function of treatment time. The mineralization rates were determined from the slopes of the curves in Fig. 5(a); WAO, 8.94×10^{-2}; CWAO, 1.61×10^{-1}; EO, 2.42×10^{-2}; and EO + EC, 8.09×10^{-2} mg L^{-1} min^{-1}. The corresponding mineralization (first order) rate constants derived from Fig. 5(b) are: $k_{,WAO}$, 9.00×10^{-4}; k_{CWAO}, 1.90×10^{-3}; k_{EO}, 2.00×10^{-4}; and k_{EO+EC}, 8.00×10^{-4} min^{-1}. The k_{CWAO} is nine times greater than k_{EO}. On the basis of initial and final TOC values, the percent TOC removals were estimated and compared in Table 3. It is found that CWAO process is more efficient with 42.4%. Only WAO (without catalyst) showed lesser efficiency (23.0%). On the other hand, EO and EC–EO treatments were found to be less efficient with 8.4 and 21.2%, respectively.

3.4. Mechanism of exchange of SA on the resin

The pH of the aqueous SA solution was found to be 4.3 ± 0.1. The experimentally observed variation of pH of eluent with increasing bed volumes is compared with the corresponding BTC in Fig. 6. This is compared with the expected pH variation with eluent bed volumes considering deprotonation of SA molecules during exchange on the resin. It is seen from Fig. 6 that the observed initial pH of eluent was about 9.2, which remained constant within the initial plateau region of BTC, thereafter, the pH decreased gradually as the SA is eluted slowly after the breakthrough point and finally leveled-off at pH 4.3, which is characteristic of aqueous SA feed solution.

At least three possible pathways for the ion-exchange of SA molecules can be imagined.

Mechanism (a): Ion-exchange involving partial deprotonation of SA molecules:

If exchange involves deprotonation of SA molecules, OH^- ions (released from resin) are neutralized by H^+ (derived from deprotonation of SA). This results in neutral pH of eluent in the initial plateau region of BTC, in which case the curve representing pH variation should have been similar to the expected pH variation (Fig. 6). The exchange reaction may be written as:

$$R^+ - OH^- + HOOC - (CH_2)_8 - COOH \rightarrow R^+ - {}^-OOC - (CH_2)_8 - COOH + H_2O \quad (2)$$

Mechanism (b): Ion-exchange without deprotonation of SA molecules:

In this case, SA molecule is exchanged on the resin without deprotonation and the OH^- ions from resin

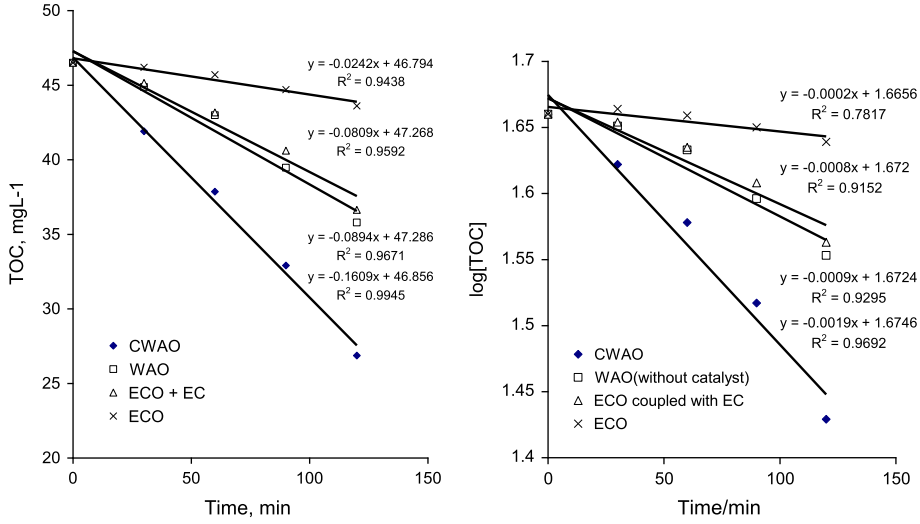

Fig. 5. (a) Kinetic plots showing TOC reduction with increase in treatment time and (b) log [TOC] vs. treatment time under CWAO, WAO, EO + EC, and EO reaction conditions.

Table 3
Comaparison of mineralization efficiencies of different oxidation processes in SA wastewater treatment

Method	Concentration of TOC (mg/L)		Mineralization (%)
	Initial	Final	
EO[a]	46.5 ± 1.7	42.6 ± 0.2	8.4
EO + EC[b]	46.5 ± 1.7	36.6 ± 0.3	21.2
WAO[c]	46.5 ± 1.7	35.8 ± 0.3	23.0
CWAO[d]	46.5 ± 1.7	26.9 ± 1.0	42.4

[a]A cylindrical single-compartment cell (2 L; Ti/RuO_2–Pt anode; SS cathode; 3A and 16 V DC; batch mode; treatment time 2 h). Effluent: 70 mg/L SA + 400 mg/L Na_2SO_4.
[b]A laboratory-scale reactor (1 L; aluminium plate anode; SS cathode; 1 A and 12 V DC; batch mode; treatment time 2 h). Effluent: 70 mg/L SA + 400 mg/L Na_2SO_4.
[c]A high pressure reactor (volume 0.5 l; temperature 473 K; Pressure 0.69 MPa; rpm 200; treatment time 2 h after attaining the operating temperature). Effluent: 70 mg/L SA + 400 mg/L Na_2SO_4.
[d]A high pressure reactor (catalyst (60%) $PdCl_2$ 8 mg; volume 0.5 l; temperature 473 K; pressure 0.69 MPa; rpm 200; treatment time 2 h after attaining the operating temperature). Effluent: 70 mg/L SA + 400 mg/L Na_2SO_4.

accumulate in the eluent, then the resulting in pH ⩾ 7. However, due to absence of counter cations (e.g. H^+ or Na^+) in solution, a mechanism involving the release of free OH ions may not be justified. Thus, the exchange reaction of SA can be assumed to involve undissociated SA molecules as shown in Eq. (4). It appears reasonable because the pH of aqueous SA solution was 4.3, which is below $pKa_1 = 4.7$ and $pKa_2 = 5.4$ of SA [3].

$$R^+–OH^- + HOOC–(CH_2)_8–COOH \rightarrow R^+–OH...HOOC–(CH_2)_8–COOH \quad (3)$$

Though the observed pH of the eluent was in the range 9.0–9.2 in the initial plateau region of the breakthrough curve, it is difficult to comprehend this observation at this stage. One possibility is that the residual NaOH present in the micro pores of the OH-form of resin gradually bleed out during the experiment and cause higher pH of eluents. However, we are at present examining this aspect in detail.

Mechanism (c): Ion-exchange with complete deprotonation of SA molecules:

An experiment was conducted in which the pH of the feed solution was increased above $pKa_2 = 5.4$ by adding NaOH, by which deprotonation of SA occurs and $^-OOC—(CH_2)_8—COO^-$ species is formed *ex situ*. In this case, due to the OH^- released from resin, the eluent pH should be >5.4 in the initial plateau region as expected from Eq. (5).

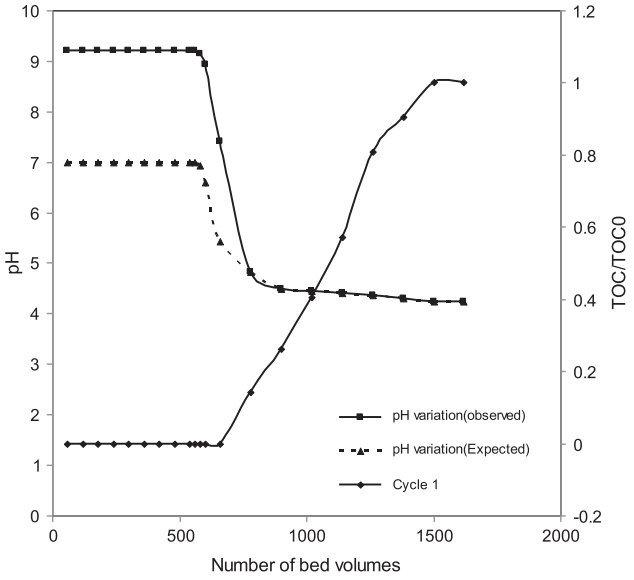

Fig. 6. Comparison of experimentally observed and expected variation of pH of eluent, with increasing eluent bed volumes. The corresponding breakthrough curve is also included.

$$R^+—OH^- + {}^- OOC—(CH_2)_8—COO^- + Na^+ \rightarrow R^+ \ldots {}^-OOC—(CH_2)_8—COO^- + 2NaOH \quad (4)$$

Therefore, from the above *ex situ* deprotonation experiment; it is concluded that the removal of SA occurs is represented by reaction step (4) involving undissociated SA molecules at pH below $pKa_1 = 4.7$, while in reaction (5) dissociated SA molecules at pH > 5.4 are involved. In reaction step (4), the exchange of SA molecules could involve electrostatic interaction between electronegative oxygen atom of polar carboxyl groups of SA and resin-bound R_3N^+ groups. The observation that the uptake of SA is strongly inhibited in the presence of inorganic anions supports such weak interaction between SA and resin. It may be appropriate to refer this mechanism as very similar to adsorption of SA. Cao et al. [15] investigated the recovery of L-(+) lactic acid by anion-exchange resin and the mechanism was described as adsorption and not ion-exchange.

It was mentioned in Section 3.2.1 that a total 560 mg SA from 8.0 L of feed solution accounts for complete saturation of resin bed. But, the actual amount of SA recovered was 510 mg, which corresponds to 0.51 g solute/8.2 ml wet resin bed. Since the equivalent weight of SA is 101 gram-equivalent, the total concentration of recovered SA is equal to 5.05 meq. However, based on the exchange capacity specified by the vendor (Table 1), the total amount of SA that can be exchanged is calculated as 11.48 meq. This value is twice that of the actually recovered concentration of SA. This implies that both the carboxylic acid groups of a SA molecule participate in the exchange reaction and each SA molecule replaces two OH groups from the surface of the resin in a dual-site exchange process. Therefore, the stoichiometry between the number of sites of exchange and SA is 2:1. Bhandari et al. [16] discussed the ion-exchange behavior of strongly polybasic acids (H_3PO_4) on weak-base resins and provided evidence for similar dual-site sorption with divalent ion HPO_4^{2-}.

3.5. Mechanism of mineralization of sebacid acid through AOPs

In the treatment of SAWW reported in Section 3.3, the mineralization efficiency was observed in the order of CWAO > WAO > EO coupled with EC > EO. Many advanced oxidation processes are based on the generation of highly reactive radical species, specially the hydroxyl radical (·OH) [17–19]. EO has been widely studied with both real and synthetic industrial wastes [19,20]. Several studies on the aqueous wastes containing carboxylic acids have been reported in the past, particularly, oxalic acid [20] and maleic acid [21,22]. The final product with diamond thin-film electrodes is carbon dioxide [23]. EO of succinic acid using boron-doped diamond electrode is recently reported [23,24]. In the present study, electrooxidation has been studied using anodes of Ti-coated with RuO_2 and doped with Pt (Ti/RuO_2–Pt). The efficiency of electrooxidation is observed to be low. SA molecule, having eight sp^3-carbons out of ten carbons present, seems to resist to electrooxidation reaction. It appears that oxidation of saturated carbons is more difficult, and hence low electro-oxidation efficiency was obtained.

We found that CWAO using Pd^{2+} catalyst yielded 42.4% mineralization efficiency. The TOC removal may be attributed to participation of reactive oxygen species, while many reaction pathways involving H-abstraction by $O_2^{\cdot-}$, H_2O-addition, decarboxylation, isomerisation, dimerization, and polymerization of organic radicals generated within the reactor are also feasible [25]. Gomes et al. [26,27] reported CWAO of refractory carboxylic acids using (1 wt.%) Pt/C with conversion efficiencies up to 60–75% at 200˚C and 6.9 bar O_2. Decarboxylation of maleic to acrylic acid followed by a series of decarboxylation and oxidation reactions to lower molecular mass acids, and eventually to CO_2 appears to be the principal reaction pathway [28]. Wet oxidation of pyruvic acid using suspended MnO_2 at is also reported [29]. WAO and CWAO of various monocarboxylic (such as formic, acetic, propionic, and butyric acids) and dicarboxylic

aliphatic acids (such as oxalic, adipic, succinic, and glutaric acids) have received a lot of attention [30]. During CWAO of stearic acid ($C_{18}H_{34}O_2$) using noble metal supported ceria, the reaction was observed to occur via successive carboxy–decarboxylation yielding essentially CO_2 [31]. If the reaction involves C–C bond rupture, a molecule of acetic acid can be produced per molecule of stearic acid besides CO_2. During CWAO of oleic acid catalyzed by ceria-supported Pt catalyst, a decarboxylation mechanism was proposed with the intermediate formation of a Cn−1 acid and CO2 at each step [32]. Noble metals, palladium, platinum, and ruthenium were found to be excellent catalysts for treating carboxylic acid [31,32].

In the present study, the EO and CWAO were applied to screen for oxidative degradation of SA wastewater in a bid to provide an alternative to the ion-exchange removal of SA, which was observed to have strong influence of sulfate ions that coexist in the real SA manufacturing wastewater. However, degradation of SA using these methods needs to be investigated in depth looking into the reported build up of low molecular weight carboxylic acids, particularly, acetic acid, in similar studies.

4. Conclusions

On the basis of results obtained in the present study it may be concluded that:

- Efficient removal of SA from aqueous solutions using strong base anion exchange resin is possible. However, the process is severely limited by the inorganic anions viz., SO_4^{2-}, HPO_4^{2-}, Cl^-, NO_3^-, which strongly compete with SA. Therefore, the IE process cannot be advantageously applied for treatment of real SA wastewater, which contains high concentrations of sodium sulfate.
- On the other hand, SA wastewater is amenable for CWAO treatment during which SA is mineralized with moderate efficiency.

Acknowledgment

The authors wish to thank Dr. S.R. Wate, Director, NEERI and Dr. T. Nandy, Chief Scientist and Head, WWT Division, NEERI for encouragement.

References

[1] F. Zhang, C. Huang, T. Xu, Production of sebacic acid using two-phase bipolar membrane electrodialysis, Ind. Eng. Chem. Res. 48 (2009) 7482–7488.
[2] Material Safety Data Sheet, Sebacic acid, CC: SLS3310, Sciencelab, Houston, Texas 77396.
[3] J.G. Speight, Lange's Handbook of Chemistry, 16th ed., McGraw Hill, New York, 2005.
[4] D.S. Ogunniyi, Castor oil: A vital industrial raw material, Bioresour. Technol. 97 (2006) 1086–1091.
[5] NEERI Report, Studies on Removal of Phenol and Associated COD from Wastewater Generated from Sebacic Acid Manufacture, 2007.
[6] A. Rubalcaba, M.E. Suarez-Ojeda, F. Stuber, A. Fortuny, C. Bengoa, I. Metcalfe, J. Font, Y. Ku, K.-C. Lee, Removal of phenols from aqueous solution by XAD-4 resin, J. Hazard. Mater. B 80 (2000) 59.
[7] N.N. Rao, J.R. Singh, R. Mishra, T. Nandy, Liquid–liquid extraction of phenol from simulated sebacic acid wastewater, J. Sci. Ind. Res. 68 (2009) 823–828.
[8] N.N. Rao, R. Misra, N. Gedam, P.N. Parameswaran, J.K. Astik, Kinetics of electrooxidation of landfill leachate in a three-dimensional carbon bed electrochemical reactor, Chemosphere 76 (2009) 1206–1212.
[9] American Public Health Association (APHA). Standard Methods for the Examination of Water and Wastewater, 19th ed., Washington, DC, 1995.
[10] M. Duncan, N.J. Horan, eds., Handbook of Water and Wastewater Microbiology, 2003, p. 168.
[11] G. Samudro, S. Mangkoedihardjo, Review on BOD, COD and BOD/COD ratio: A triangle zone for toxic, biodegradable and stable levels, Int. J. Acad. Res. 2(4) (2010) 235–239.
[12] M.M.F. Garcia-Soto, E.M. Camacho, Boron removal from industrial wastewaters by ion exchange: An analytical control parameter, Desalination 181 (2005) 207–216.
[13] T. Nur, M.A.H. Johir, P. Loganathan, S. Vigneswaran, J. Kandasamy, Effectiveness of Purolite A500PS and A520E ion exchange resins on the removal of nitrate and phosphate from synthetic water, Desalin. Water Treat. 47 (2012) 50–58.
[14] F.I. Hai, K. Yamamoto, K. Fukushi, Hybrid treatment systems for dye wastewater, Crit. Rev. Environ. Sci. Technol. 37 (2007) 315–377.
[15] X. Cao, H.S. Yun, Y.-M. Koo, Recovery of L-(+)-lactic acid by anion exchange resin Amberlite IRA-400, Biochem. Eng. J. 11 (2002) 189–196.
[16] V.M. Bhandari, V.A. Juvekar, S. Patwardhan, Ion-exchange studies in the removal of polybasic acids. Anomalous sorption behavior of phosphoric acid on weak base resins, Sep. Sci. Technol. 32 (1997) 2481–2496.
[17] G. Chen, Electrochemical technologies in wastewater treatment, Sep. Purif. Technol. 38 (2004) 11–41.
[18] Y. Deng, J.D. Englehardt, Electrochemical oxidation for landfill leachate treatment, Waste Manage. 27 (2007) 380–388.
[19] N.N. Rao, K.M. Somasekhar, S.N. Kaul, L. Szpyrkowicz, Electrochemical oxidation of tannery wastewater, J. Chem. Technol. Biotechnol. 76 (2001) 1124–1131.
[20] C.A. Martínez-Huitle, S. Ferro, A. De Battisti, Electrochemical incineration of oxalic acid: Reactivity and engineering parameters, J. Appl. Electrochem. 35 (2005) 1087–1093.
[21] E. Weiss, K. Groenen-Serrano, A. Savall, C. Comninellis, A kinetic study of the electrochemical oxidation of maleic acid on boron-doped diamond, J. Appl. Electrochem. 37 (2007) 41–47.
[22] P. Canizares, J. García-Gómez, J. Lobato, M.A. Rodrigo, Electrochemical oxidation of aqueous carboxylic acid wastes using diamond thin-film electrodes, Ind. Eng. Chem. Res. 42 (2003) 956–962.
[23] N. Bensalah, B. Louhichi, A. Abdel-Wahab, Electrochemical oxidation of succinic acid in aqueous solutions using boron doped diamond anodes, Int. J. Environ. Sci. Technol. (Available, online, 27 October 2011).
[24] E. Brillas, I. Sirés, P. Lluís Cabot, Use of both anode and cathode reactions in wastewater treatment, in: Electrochemistry for the Environment, 2010, pp. 515–552.
[25] F. Stubera, J. Font, A. Fortuny, C. Bengoa, A. Eftaxias, A. Fabregat, Carbon materials and catalytic wet air oxidation of organic pollutants in wastewater, Topics Catal. 33 (2005) 3–50.

[26] H.T. Gomes, P. Serp, P. Kalck, J.L. Figueiredo, J.L. Faria, Carbon supported platinum catalysts for catalytic wet air oxidation of refractory carboxylic acids, Topics Catal. 33 (2005) 59–68.
[27] H.T. Gomes, J.L. Figueiredo, J.L. Faria, Catalytic wet air oxidation of low molecular weight carboxylic acids using a carbon supported platinum catalyst, Appl. Catal. B Environ. 27 (2000) L213–L217.
[28] L. Oliviero, J. Barbier Jr., D. Duprez, H.W. Jack, W. Ponton, I.S. Metcalfe, D. Mantzavinos, Wet air oxidation of aqueous solutions of maleic acid over Ru/CeO_2 catalysts, Appl. Catal. B: Environ. 35 (2001) 1–12.
[29] R. Andreozzia, V. Capriob, A. Insolaa, R. Marottab, V. Tufanoc, The ozonation of pyruvic acid in aqueous solutions catalyzed by suspended and dissolved manganese, Water Res. 32 (1998) 1492–1496.
[30] V.S. Mishra, V.V. Mahajani, J.B. Joshi, Wet air oxidation, Ind. Eng. Chem. Res. 34 (1995) 2–48.
[31] B. Renard, J. Barbier, Jr., D. Duprez, S. Durecu, Catalytic wet air oxidation of stearic acid on cerium oxide supported noble metal catalysts, Appl. Catal. B: Environ. 55 (2005) 1–10.
[32] B. Levasseur, B. Renard, J. Barbier, Jr., D. Duprez, Catalytic wet air oxidation of oleic acid on ceria supported platinum catalyst. Effect of pH, React. Kinet. Catal. Lett. 87 (2006) 269–279.